Planar Dual-Band Branch-Line Coupler With Large Frequency Ratio

LEI XIA [1], **JIA-LIN LI** [2], **BAIDENGER AGYEKUM TWUMASI** [2,3], **PENG LIU** [2], **AND SHAN-SHAN GAO** [4]

[1] School of Electronic Science and Engineering, University of Electronic Science and Technology of China, Chengdu 611731, China
[2] School of Physics, University of Electronic Science and Technology of China, Chengdu 610054, China
[3] Electrical/Electronic Engineering Department, Ho Technical University, Ho, Ghana
[4] School of Electronic and Information Engineering, Chengdu University, Chengdu 610106, China

Corresponding author: Jia-Lin Li (jialinli@uestc.edu.cn)

ABSTRACT This work presents a novel planar branch-line coupler topology developed for dual-band operation using an E-shaped impedance transformer network to supplant the conventional microstrip line. Explicit closed-form design equations for dual-band operation are derived using the ABCD matrices. The studied coupler features a large dual-band frequency ratio with a compact size. A prototype coupler centered at 1 and 8 GHz is first presented and experimentally examined to demonstrate the large frequency ratio. Further, another prototype coupler centered at 2.4 and 5.2 GHz for potential WLAN applications is also developed and experimentally characterized. Measurements and simulations for both prototype couplers show good performance within the studied dual-band frequencies.

INDEX TERMS Dual-band, branch-line coupler, E-shaped impedance transformer, large frequency ratio.

I. INTRODUCTION

The importance of microstrip branch-line couplers in microwave/radio frequency components and many applications have been as a result of the increase in multi-band components and system applications [1]–[8]. This notwithstanding, the branch-line coupler is still a prevalent microwave component till date as multi-band systems continue to evolve. Recently, dual-band communication systems have been on the increase, resulting in high demand for dual-band components such as branch-line couplers. The branch-line coupler with equal or unequal power division is one of the basic components commonly used in microwave engineering for dual-band applications.

For the design of branch-line couplers with dual-band operations, early work was reported by using π-shaped network [9], and recently by using the coupled-line stub based π-shaped structure [10]. Equivalently, the π-shaped structure can be replaced by a T- or cross-shaped stub loading, as studied in [11], [12]. On the other hand, the coupled transmission line (TL) and coupled π-shaped network were found to function as the dual-band responses [6], [13], [14]. Other techniques such as dual TL [15], embedded metamaterial

The associate editor coordinating the review of this manuscript and approving it for publication was Haiwen Liu [ ].

based electromagnetic bandgap (EBG) [16] or composite right/left-handed (CRLH) TL [17] have also been reported for designing the dual-band couplers. Further designs reported the parallel combination of coupled line and TL [18], port extension [19], coupled lines [20], [21], and so on. In [10], coupled line based quarter-wavelength opened/ shorted stub modification was made to the conventional branch-line coupler to realize dual/tri-band operations, where the achieved frequency ratio is small, while the circuit is complex and bulky. In [12], a cross-shaped stub branch-line coupler is presented for dual-band applications with a wide frequency ratio. Further, extending the frequency ratio and reducing the circuit size for such components will be very much appreciated for current and future microwave systems. In [22] a compact dual-band rat-race coupler with enhanced bandwidth has been proposed but the frequency ratio needs to be further extended. By meandering the high-impedance segments of the stepped impedance stubs, as compared to conventional realization, the miniaturization is achieved. A miniaturized dual-band branch-line coupler proposed in [23] features about 75% size reduction by meandering the TL section, but the frequency ratio is also not large. In [24], a novel directive coupler with dual-band performance is proposed for GSM applications. The coupler has good dual-band performance with a phase imbalance less than one degree but the frequency

ratio is relatively small. In [25], a novel dual-band branch-line coupler with high isolation using coupled lines is proposed. The achieved frequency ratio for this coupler is not wide enough though featuring high isolation and simple structure.

The above studies demonstrate the function of dual-band operations, but in general, the dual-band frequency ratio is small. It is believed that to further facilitate the potential applications in modern wireless communications, enlarging the frequency ratio with a compact circuit size without compromising the performance is of great importance.

In this paper, a novel compact branch-line coupler topology is proposed based on E-shaped impedance transformer network to supplant the conventional transmission line for dual-band operations. Closed-form design equations are derived to develop the proposed branch-line coupler. Demonstration on a dual-band coupler with a large frequency ratio of 1 and 8 GHz is first presented and experimentally examined; and further a prototype demonstrator coupler centered at 2.4/5.2 GHz for potential WLAN applications is designed and implemented based on this study. Experimental examinations on the prototype couplers show good agreement with the simulation results, thus confirming the study of this work.

II. STRUCTURE AND THEORY OF THE PROPOSED DUAL-BAND BRANCH-LINE COUPLER

A conventional branch-line coupler consists of four quarter-wavelength impedance transformers. In general, the dual-band function can be implemented by using dual-band impedance transformers. The schematic diagram of an E-shaped network for dual-band applications together with a standard quarter-wavelength line is shown in Fig. 1. The E-shaped network comprises of series TLs with normalized characteristic impedances of z_s and two symmetrically placed shunt stubs of normalized characteristic impedances of z_p as well as a centrally loaded shunt stub with a normalized characteristic impedance of $z_p/2$, where all TL sections have the electric lengths of 90° at f_0. Here f_0 is defined as the arithmetical average of the two frequency bands.
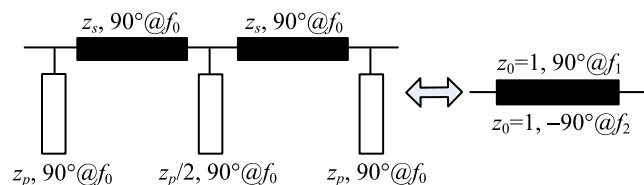

FIGURE 1. The studied E-shaped network and equivalent quarter-wavelength line, where 90° is referred to $f_0 = (f_1 + f_2)/2$.

Actually, the presented network can be viewed as two cascaded π-shaped networks, where each π-shaped network has normalized characteristic impedances of z_s for the series TL and z_p for the shunt stubs. By cascading, the centrally loaded two stubs can be further combined into one stub, thus its characteristic impedance is halved, leading to the studied E-shaped network.

The above E-shaped network can be analyzed based on the ABCD-matrix formulation, given by

$$\begin{bmatrix} A_E & B_E \\ C_E & D_E \end{bmatrix} = \begin{bmatrix} A^2 - BC & jB(A+D) \\ jC(A+D) & D^2 - BC \end{bmatrix} \quad (1)$$

where

$$A = D = \cos \frac{\pi f}{2f_o} - yz_s \sin \frac{\pi f}{2f_o} \quad (2)$$

$$B = z_s \sin \frac{\pi f}{2f_o} \quad (3)$$

$$C = \sin \frac{\pi f}{2f_o} \left(\frac{1}{z_s} - z_s y^2 + 2y \cot \frac{\pi f}{2f_o} \right) \quad (4)$$

Now, let the E-shaped network be equivalent to a quarter-wavelength line with 90° at f_1 and −90° at f_2 ($f_1 < f_2$), leading to

$$z_s = \frac{1}{\sqrt{2} \sin \frac{\pi}{1+k}} \quad (5)$$

where k is the frequency ratio of the dual-frequency band, i.e. $k = f_2/f_1$. The characteristic impedance of the stub is given by

$$z_P = -\frac{\sqrt{2} \cot \left(\frac{\pi}{1+k} \right)}{2 \cos \left(\frac{\pi}{1+k} \right) - \sqrt{2}} \quad (6)$$

for a short stub when $1 < k < 3$. And

$$z_P = \frac{\sqrt{2} \tan(\frac{\pi}{1+k})}{2 \cos \left(\frac{\pi}{1+k} \right) - \sqrt{2}} \quad (7)$$

for an open stub when $k > 3$.

Fig. 2 shows the layout of the proposed dual-band coupler with all branch lines replaced by the E-shaped network. It is seen from Fig. 2 that all stubs are directed towards the inner area of the structure emanating from the inner corners to realize a compact circuit area. From Fig. 2, z_{s1} and z_{s2} are further specified as

$$z_{s1} = \frac{1}{2 \sin \frac{\pi}{1+k}} \quad (8)$$

$$z_{s2} = \frac{1}{\sqrt{2} \sin \frac{\pi}{1+k}} \quad (9)$$

While for z_{p1}, z_{p2} and z_{p3}, they are modified as

$$z_{p1} = \frac{-\cot \frac{\pi}{1+k}}{\left(4 \cos \frac{\pi}{1+k} - 2\sqrt{2} \right)} \quad (10)$$

$$z_{p2} = \frac{-\sqrt{2} \cot \frac{\pi}{1+k}}{\left(4 \cos \frac{\pi}{1+k} - 2\sqrt{2} \right)} \quad (11)$$
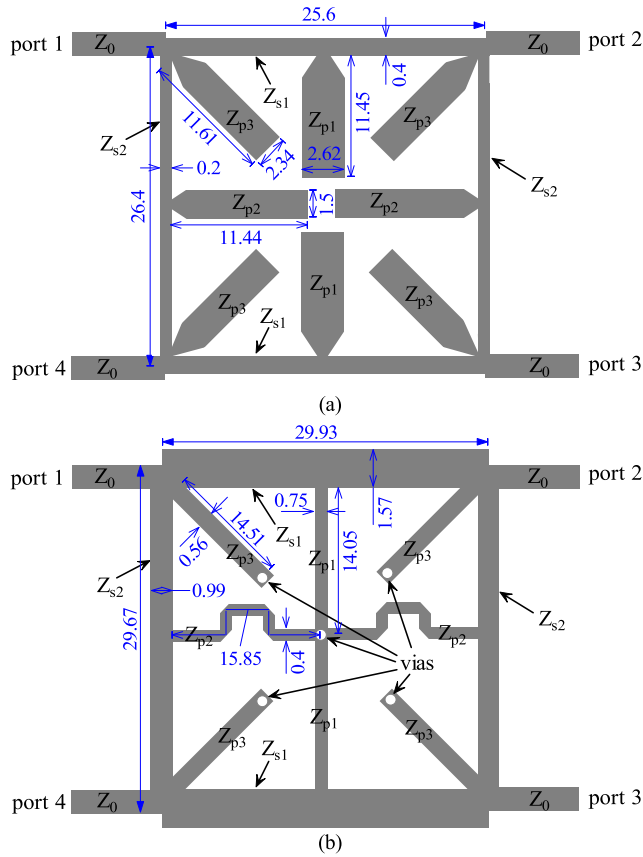
FIGURE 2. Layout of the proposed dual-band branch-line coupler. (a) $f_1 = 1$ GHz, $f_2 = 8$ GHz, i.e. $k > 3$, and all stubs of the E-shaped network are open-circuited. (b) $f_1 = 2.4$ GHz, $f_2 = 5.2$ GHz, namely $k < 3$, and all stubs of the E-shaped network are short-circuited.

$$z_{p3} = \frac{-\sqrt{2}\cot\dfrac{\pi}{1+k}}{\left(2\cos\dfrac{\pi}{1+k} - \sqrt{2}\right)\left(1+\sqrt{2}\right)} \tag{12}$$

for short stubs when $1 < k < 3$; and

$$z_{p1} = \frac{\tan\dfrac{\pi}{1+k}}{\left(4\cos\dfrac{\pi}{1+k} - 2\sqrt{2}\right)} \tag{13}$$

$$z_{p2} = \frac{\sqrt{2}\tan\dfrac{\pi}{1+k}}{\left(4\cos\dfrac{\pi}{1+k} - 2\sqrt{2}\right)} \tag{14}$$

$$z_{p3} = \frac{\sqrt{2}\tan\dfrac{\pi}{1+k}}{\left(2\cos\dfrac{\pi}{1+k} - \sqrt{2}\right)\left(1+\sqrt{2}\right)} \tag{15}$$

for open stubs when $k > 3$.

Fig. 3 shows the normalized $z_{s1}, z_{s2}, z_{p1}, z_{p2}$ and z_{p3} as a function of the frequency ratio k. It is seen that the proposed dual-band branch-line coupler can operate at a wide range of frequency ratios of 1.75-2.4 and 3.95-8
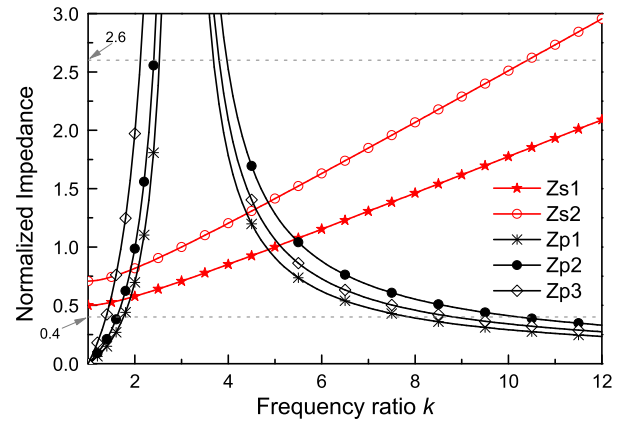

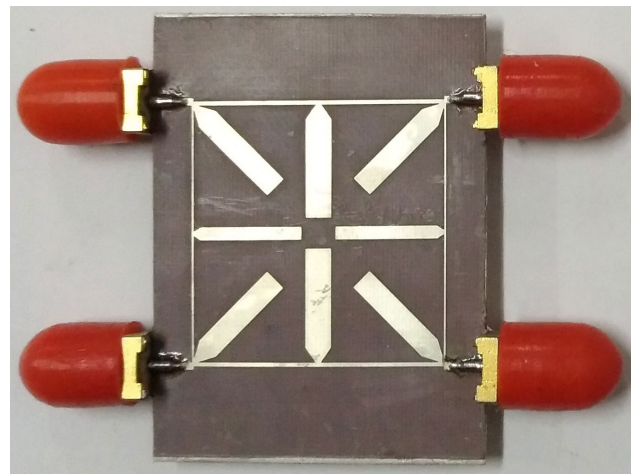**FIGURE 3.** Normalized characteristic impedances against frequency ratio k.

FIGURE 4. Photograph of the fabricated 1/8-GHz dual-band prototype coupler, where the detailed dimensions are shown in Fig. 2(a).

when referred to the microstrip-line implementation with normalized characteristic impedances from approximately 0.4 to 2.6.

III. DEMONSTRATION ON A BRANCH-LINE COUPLER WITH LARGE FREQUENCY RATIO OF 1 AND 8 GHZ

The first prototype demonstrator is a dual-band coupler with a large frequency ratio, specified as 1 and 8 GHz, as shown in Fig. 2(a). Since the frequency ratio is $k = 8$, except (8) and (9), Equations (13)-(15) are utilized to evaluate the line impedances; the normalized impedances are respectively $z_{s1} = 1.462$, $z_{s2} = 2.067$, $z_{p1} = 0.391$, $z_{p2} = 0.553$ and $z_{p3} = 0.429$. After de-normalization referred to a 50Ω system, these are respectively 73.1 Ω, 103.35 Ω, 19.55 Ω, 27.65 Ω and 21.45 Ω, while $f_0 = 4.5$ GHz. The prototype coupler is developed on a laboratory-available microwave substrate with a relative permittivity of $\varepsilon_r = 2.2$ and a thickness of 0.25 mm as well as a loss tangent of 0.001; Fig. 2(a) shows the layout, where each open-circuited stub
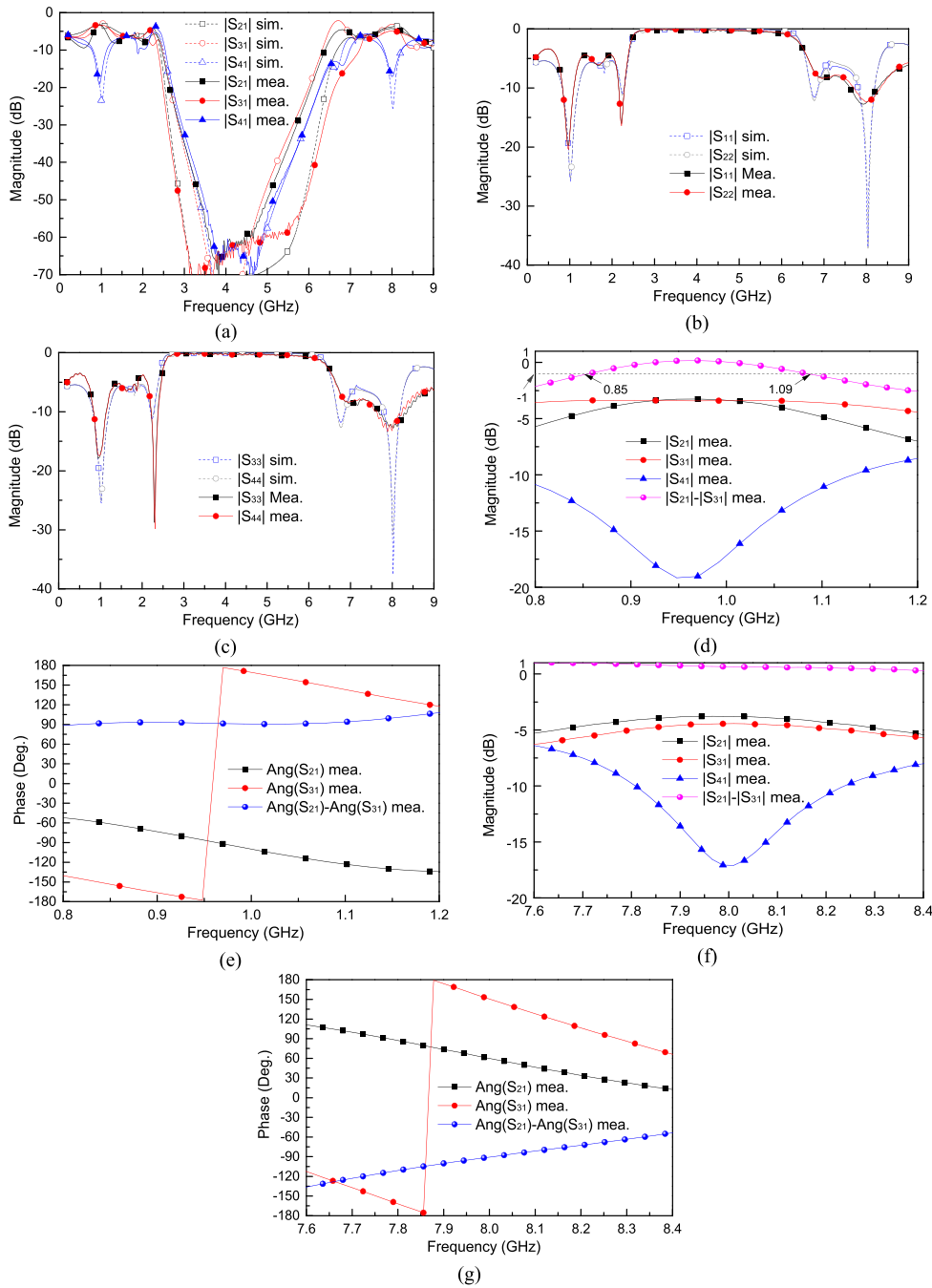
FIGURE 5. Performance of the developed 1/8-GHz dual-band prototype coupler. (a) Through $|S_{21}|$, coupling $|S_{31}|$ and isolation $|S_{41}|$. (b) Return losses for ports 1 and 2. (c) Return losses for ports 3 and 4. (d) In-band magnitude response at the lower band. (e) In-band phase response at the lower band. (f) In-band magnitude response at the upper band. (g) In-band phase response at the upper band.

is tapered at the T-junction to more accurately model the loading position of the E-shaped network. Based on the above calculated parameters, the electric performance of such a coupler is numerically analyzed by using a full-wave electromagnetic simulator, Ansoft Ensemble 8.0, to fully involve the junction discontinuities. After optimal designs, the physical dimensions are found as (units: mm): 0.4 for 73.1 Ω, 0.2 for

103.35 Ω, 2.62 for 19.55 Ω, 1.5 for 27.65 Ω and 2.34 for 21.45 Ω, while the lengths for horizontal and vertical arms of the coupler are 25.6 and 26.4 mm. The loaded stub lengths for z_{p1}, z_{p2} and z_{p3} are 11.45, 11.44 and 11.61 mm, respectively. These dimensions are also marked in Fig. 2(a).

The developed 1/8-GHz prototype coupler is fabricated; shown in Fig. 4 is the photograph of such a demonstrator.

The measurements were carried out by using a vector network analyzer, Agilent N9918A, with full two-port calibrations. Figs. 5(a)-(g) record the achieved performance both from measurements and from simulations. The wideband response is shown in Figs. 5(a)-(c). From the transmission (through) $|S_{21}|$, the coupling $|S_{31}|$ and the isolation $|S_{41}|$ shown in Fig. 5(a), one can see the response exhibits wideband notch between the two frequency bands. Meanwhile, the measured $|S_{21}|$ and $|S_{31}|$ are -3.35 dB and -3.4 dB at 0.95 GHz, and -3.87 dB and -4.5 dB at 8 GHz, respectively, while the isolations at the two bands are better than 17 dB. It is believed the slightly higher losses at the upper band can be primarily due to the losses of utilized SMA connectors and the back-to-back transition between microstrip line and the connector that is to enable the measurements. Also, the higher loss may be due to the higher conductor loss at the higher frequencies since we use the Tin-plated strip to avoid rust. From Figs. 5(b) and (c), it is found the impedance matchings at all ports are good, where return losses over 15 dB at the lower frequency band are observed from measurements, while they are better than 12 dB at the upper frequency band. Notice that the two spurious resonances at approximately 2.2 and 6.6 GHz, respectively, maybe result from the junction discontinuities, leading to unequal couplings between ports 2 and 3, where the through port, S_{21}, is dominant while the coupling port, S_{31}, is secondary at the lower spurious resonance, while it is opposite at the upper spurious resonance. The two spurious resonances are not the desired passbands since they are not designable and controllable based on the presented analyses, hence the demonstrator basically behaves the dual-band responses. Further, Fig. 5(d) depicts the measured in-band response at the lower band. It shows the measured center frequency is slightly shifted to approximately 0.95 GHz, and by referring to a magnitude imbalance of 1 dB, the bandwidth can cover from 0.85 to 1.09 GHz, indicating a relative bandwidth of 25.3%. The phase response for this case is shown in Fig. 5(e), where by referring to a phase imbalance of $\pm5°$, a frequency band from 0.78 to 1.11 GHz is observed. The upper band responses are recorded in Figs. 5(f) and (g). Under the same magnitude imbalance of 1 dB, the corresponding bandwidth is ranged from 7.29 to 8.91 GHz, thus formulating a relative bandwidth of 20.3%, whereas the measured phase bandwidth is 215 MHz as compared with the simulations of 280 MHz under a phase imbalance of $\pm5°$. It is noted the phase bandwidth can be widened by using phase compensation techniques, as reported in [26].

In general, the above measurements are in good agreement with the predications. The achieved performance also confirms the presented topology can be utilized to design a dual-band coupler with large frequency ratios.

IV. DEMONSTRATION ON A 2.4/5.2-GHZ DUAL-BAND COUPLER FOR WLAN APPLICAITONS

For further demonstration purposes, a microstrip dual-band coupler centred at 2.4/5.2 GHz for potential WLAN applications is developed as described in Fig. 2(b), where the
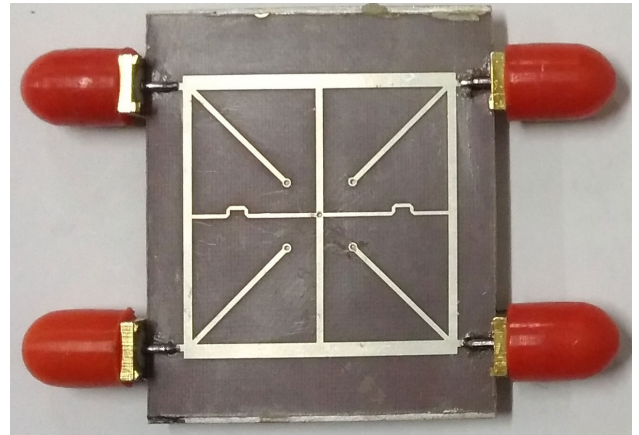

FIGURE 6. Photograph of the developed 2.4/5.2-GHz dual-band coupler, where the detailed dimensions are shown in Fig. 2(b).

loaded stubs along the horizontal and vertical arms of the coupler are short-circuited to the center position, and the horizontal stubs, corresponding to the line impedance of z_{p2}, are meandered to facilitate the required length. Based on the analyses in Section II, Equations (8)-(12) are employed in this case, where the normalized line impedances are found to be $z_{s1} = 0.596$, $z_{s2} = 0.844$, $z_{p1} = 1.02$, $z_{p2} = 1.442$ and $z_{p3} = 1.194$, respectively. Thus the corresponding de-normalized line impedances are 29.8 Ω, 42.2 Ω, 51 Ω, 72.1 Ω and 59.7 Ω; and $f_0 = 3.8$ GHz. With full-wave electromagnetic simulations, the coupler is optimally designed and fabricated on the same microwave substrate mentioned in Section III. The dimension parameters can be found as shown in Fig. 2(b). It is seen the microstrip-line widths and lengths for the horizontal and vertical arms of such a coupler are respectively 1.57 mm, 0.99 mm and 29.93 mm, 29.67 mm, while the loaded short-circuited stubs have the width and length of 0.75 mm and 14.05 mm for z_{p1}, 0.4 mm and 15.85 mm for z_{p2}, and 0.56 mm and 14.51 mm for z_{p3}, respectively, whereas all short-circuited vias have the same radius of 0.3 mm.

Photograph of the developed coupler is shown in Fig. 6. Also, the measurements were carried out by using the same vector network analyzer, Agilent N9918A. Figs. 7(a)-(g) display the measured and simulated results. The wideband responses are illustrated in Figs. 7(a)-(c). It is seen the response exhibits dual passband as expected. The measured $|S_{21}|$ and $|S_{31}|$ are respectively -3.41 dB and -3.4 dB at 2.27 GHz, and -3.51 dB and -3.97 dB at 5.05 GHz; meanwhile the isolations at the two bands are better than 30 dB and 20 dB, respectively. Both the port matching and port isolation can be clearly identified at the two predicated frequency bands. Moreover, return losses over 20 dB are measured for all ports as depicted in Figs. 7(b) and (c). The in-band responses at the lower frequency band show the demonstrator has a 1-dB magnitude imbalance bandwidth from 2.105 to 2.468 GHz, as presented in Fig. 7(d). The measured bandwidth for $\pm5°$ phase imbalance is ranged from
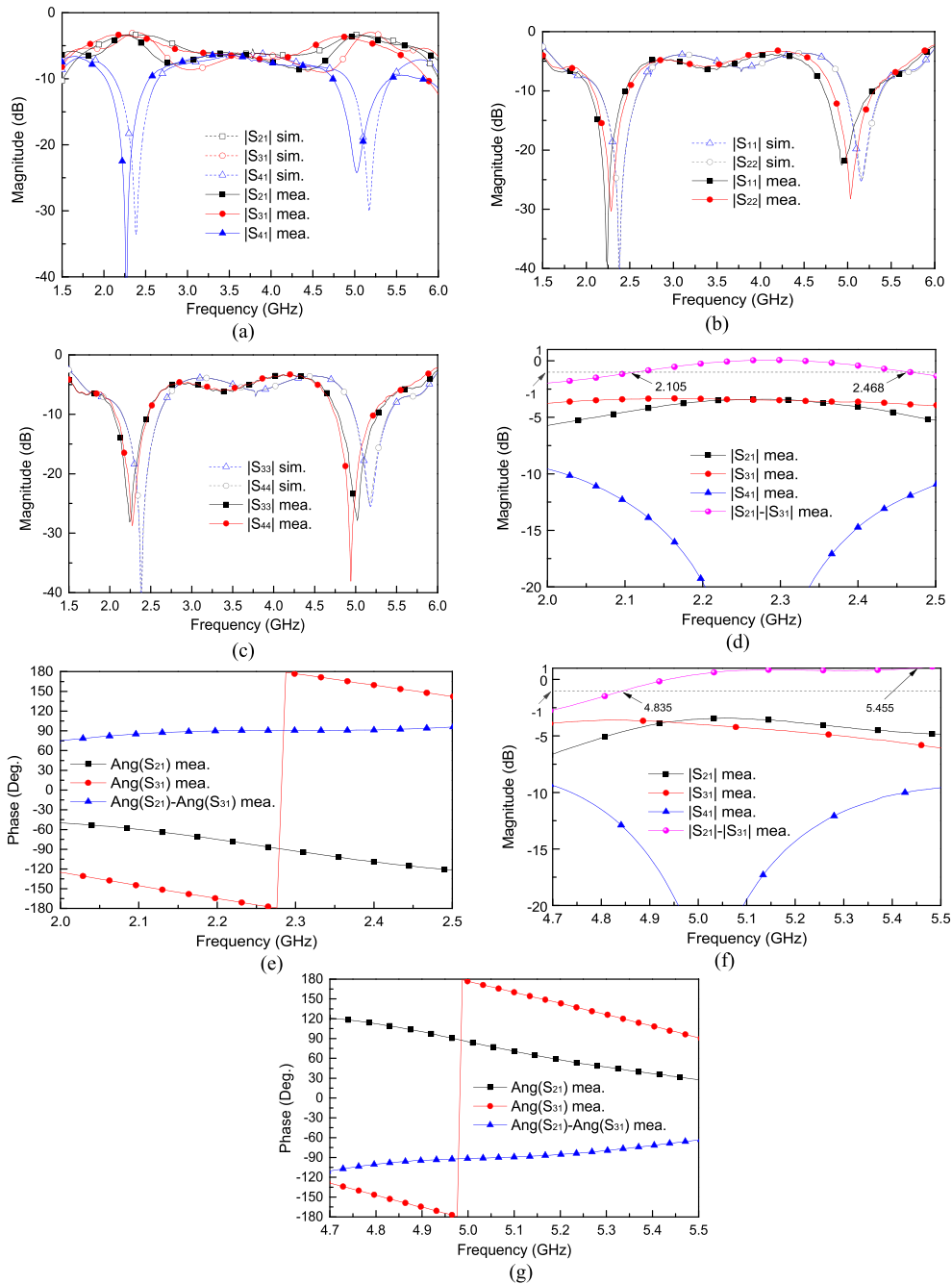
FIGURE 7. Simulated and measured results of the developed 2.4/5.2-GHz dual-band coupler. (a) Through $|S_{21}|$, coupling $|S_{31}|$ and isolation $|S_{41}|$. (b) Return losses for ports 1 and 2. (c) Return losses for ports 3 and 4. (d) In-band magnitude response at the lower band. (e) In-band phase response at the lower band. (f) In-band magnitude response at the upper band. (g) In-band phase response at the upper band.

2.096 to 2.49 GHz, as shown in Fig. 7(e). For the upper band, by referring to the same magnitude and phase imbalances, the measured bandwidths are 620 MHz shown in Fig. 7(f), and 325 MHz as described in Fig. 7(g), respectively.

The above results also indicate that the developed prototype works well based on the achieved performance. For further comparisons, Table 1 lists some reported dual-band couplers and the proposed prototypes. It is seen that most reports are of relatively small frequency ratios. The contribution in [13] can present a large frequency ratio of 11.8, but in terms of k_{max}/k_{min}, it is degraded. The studied coupler topology features a large frequency ratio, and approaches a largest k_{max}/k_{min} value of 4.57 as tabulated in Table 1.

TABLE 1. Comparisons of proposed dual-band coupler with some previously reported designs.

Refs./Years	Operation frequencies (GHz)	Magnitude bandwidth (MHz) [a]	Phase bandwidth (MHz) [b]	$\lvert S_{21}\rvert$ (dB)	$\lvert S_{31}\rvert$ (dB)	Isolation (dB)	Achievable frequency ratio, k	k_{max}/k_{min}	Techniques	Planar structure
[13]/2019	0.7/4.9	–	–	−3.57/−3.61	−3.51/−3.66	17/13	2.9-11.8	4.07	Coupled π-shaped network	Yes
[14]/2018 [c]	2.4/3.5	–	–	−2/−2.5	−5/−4	> 20/> 20	1.458	1.458	Same with the above	No (3 layers)
[15]/2016	0.85/1.8	101/228	112/220	−3.3/−3.09	−3.67/−3.9	34/19.9	1.5-4.1	2.733	π-shaped dual TL	Yes
[16]/2018	1.228/1.575	–	–	−2.9/−6.5	−3.9/−5.8	> 20/15	2.1-5.7	2.714	Embedded EBG	Yes
[17]/2016	0.93/1.78	–	–	−4.28/−3.64	−4.37/−4.3	19.7/31.8	–	1.91	CRLH TL	Yes
[21]/2013 [d]	2.45/6.17	–	–	−4.8/−6	−2.2/−3.2	> 16/> 16	2.5	–	Coupled line	Yes
[24]/2015	0.93/1.78	–	–	−3.45/−3.39	−3.46/−3.4	> 30/ > 30	1.914	–	Dual-CRLH TL	Yes
[25]/2018	0.756/1.42	–	–	−3.35/−4	−3.74/−4.1	> 15/ > 15	1.878	–	Coupled line	Yes
This work	1/8	240/1620	330/215	−3.35/−3.87	−3.4/−4.5	> 17/> 17	1.75-2.4 and 3.95-8	4.57	E-shaped network	Yes
	2.4/5.2	363/620	394/325	−3.41/−3.51	−3.4/−3.97	> 30/> 20				

Refs.	[13]	[14]	[15]	[16]	[17]	[21]	[24]	[25]	This work
ε_r	2.33	3	2.2	10.2	3.2	3.55	3	2.65	2.2
h (mm)	0.787	0.254/0.508/0.508	1.0	1.524	0.787	0.508	0.508	1.0	0.25
L×W [e]	43.52×45.62	–	31×31	27.8×23.5	52×56	21.8×23.6	–	–	25.8×26.8 / 30.92×31.24

[a] referred to 1-dB magnitude imbalance; [b] referred to ±5° phase imbalance; [c] only for simulations; [d] unequal power division with k = 1.414; [e] Length×Width in mm.

V. CONCLUSION

A novel branch-line coupler topology with large frequency ratio and its closed-form design equations for dual-band applications have been presented in this paper. Advantages of the developed dual-band coupler include large frequency ratios, compact topology, planar layout, good performance and simple design methodology. Demonstrations on two prototype couplers respectively for 1/8-GHz and 2.4/5.2-GHz operations have shown good agreement between simulations and measurements, thus validating the effectiveness of this study. It is believed that the studied coupler topology could be potential for further development towards practical applications in the dual-band microwave systems.

REFERENCES

[1] B. A. Twumasi and J.-L. Li, "Numerical simulation study on bowtie antenna-based time reversal mirror for super-resolution target detection," *J. Electr. Eng.*, vol. 70, no. 3, pp. 236–243, Jun. 2019.

[2] S.-Y. Yin, J.-L. Li, C.-G. Sun, and H. Li, "Dual-band rat-race hybrid with phase compensation," *Electromagnetics*, vol. 38, no. 3, pp. 200–206, Apr. 2018.

[3] S. Koziel and P. Kurgan, "Low-cost optimization of compact branch-line couplers and its application to miniaturized Butler matrix design," in *Proc. 44th Eur. Microw. Conf.*, Rome, Italy, Oct. 2014, pp. 227–230.

[4] B. A. Twumasi and L. Jia-Lin, "Bowtie antenna TRM design for biomedical imaging using electromagnetic time reversal technique," in *Proc. Int. Conf. Microw. Millim. Wave Technol. (ICMMT)*, Chengdu, China, May 2018, vol. 1, no. 1, pp. 60–62.

[5] J. Wu and K. Sarabandi, "Compact omnidirectional circularly polarized antenna," *IEEE Trans. Antennas Propag.*, vol. 65, no. 4, pp. 1550–1557, Apr. 2017.

[6] L. K. Yeung, "A compact dual-band 90° coupler with coupled-line sections," *IEEE Trans. Microw. Theory Techn.*, vol. 59, no. 9, pp. 2227–2232, Sep. 2011.

[7] Y.-K. Jung and B. Lee, "Dual-band circularly polarized microstrip RFID reader antenna using metamaterial branch-line coupler," *IEEE Trans. Antennas Propag.*, vol. 60, no. 2, pp. 786–791, Feb. 2012.

[8] O. Haraz, M. M. M. Ali, A. Elboushi, and A.-R. Sebak, "Four-element dual-band printed slot antenna array for the future 5G mobile communication networks," in *Proc. IEEE Int. Symp. Antennas Propag. USNC/URSI Nat. Radio Sci. Meeting*, Vancouver, BC, Canada, Jul. 2015, pp. 1–2.

[9] K. K. M. Cheng and F. L. Wong, "A novel approach to the design and implementation of dual-band compact planar 90° branch-line coupler," *IEEE Trans. Microw. Theory Techn.*, vol. 52, no. 11, pp. 2458–2463, Nov. 2004.

[10] W. Feng, Y. Zhao, W. Che, H. Chen, and W. Yang, "Dual-/Tri-band branch line couplers with high power division isolation using coupled lines," *IEEE Trans. Circuits Syst. II, Exp. Briefs*, vol. 65, no. 4, pp. 461–465, Apr. 2018.

[11] M.-J. Park, "Dual-band, unequal length branch-line coupler with center-tapped stubs," *IEEE Microw. Wireless Compon. Lett.*, vol. 19, no. 10, pp. 617–619, Oct. 2009.

[12] H. Zhang, W. Kang, and W. Wu, "A novel compact dual-band branch-line coupler with cross-shaped stubs," in *Proc. IEEE Int. Conf. Ubiquitous Wireless Broadband (ICUWB)*, Nanjing, China, Oct. 2016, pp. 1–4.

[13] A. M. Zaidi, M. T. Beg, B. K. Kanaujia, K. Srivastava, and K. Rambabu, "A dual band branch line coupler with wide frequency ratio," *IEEE Access*, vol. 7, pp. 25046–25052, 2019.

[14] L. Ma, Y. Wu, K. Zhu, Q. Yang, Z. Lai, and Y. Liu, "Multilayer compact dual-band branch-line coupler using coupled line and open-ended stub for mobile phone application: (Invited Paper)," in *Proc. Int. Appl. Comput. Electromagn. Soc. Symp. (ACES)*, Beijing, China, Jul. 2018, pp. 4–5.

[15] C. Gai, Y.-C. Jiao, and Y.-L. Zhao, "Compact dual-band branch-line coupler with dual transmission lines," *IEEE Microw. Wireless Compon. Lett.*, vol. 26, no. 5, pp. 325–327, May 2016.

[16] S. Barth and A. K. Iyer, "A dual-band quadrature hybrid coupler using embedded MTM-EBGs," in *Proc. IEEE Int. Symp. Antennas Propag. USNC/URSI Nat. Radio Sci. Meeting*, Boston, MA, USA, Jul. 2018, pp. 199–200.

[17] Q. Wang, J. Lim, and Y. Jeong, "Design of a compact dual-band branch line coupler using composite right/left-handed transmission lines," *Electron. Lett.*, vol. 52, no. 8, pp. 630–631, Apr. 2016.

[18] A. M. Zaidi, S. A. Imam, B. K. Kanaujia, and K. Rambabu, "A new equal power quadrature branch line coupler for dual-band applications," *Prog. Electromagn. Res. Lett.*, vol. 74, pp. 61–67, Jan. 2018.

[19] H. Kim, B. Lee, and M.-J. Park, "Dual-band branch-line coupler with port extensions," *IEEE Trans. Microw. Theory Techn.*, vol. 58, no. 3, pp. 651–655, Mar. 2010.

[20] A. M. Zaidi, S. A. Imam, B. K. Kanaujia, K. Rambabu, K. Srivastava, and M. T. Beg, "A new dual band 4 × 4 butler matrix with dual band 3 dB quadrature branch line coupler and dual band 45° phase shifter," *AEU-Int. J. Electron. Commun.*, vol. 99, pp. 215–225, Feb. 2019.

[21] C.-H. Yu and Y.-H. Pang, "Dual-band unequal-power quadrature branch-line coupler with coupled lines," *IEEE Microw. Wireless Compon. Lett.*, vol. 23, no. 1, pp. 10–12, Jan. 2013.

[22] A. Bekasiewicz, S. Koziel, and W. Zieniutycz, "On design optimization of miniaturized microscrip dual-band rat-race coupler with enhanced bandwidth," in *Proc. 21st Int. Conf. Microw., Radar Wireless Commun. (MIKON)*, Krakow, Poland, May 2016, pp. 1–4.

[23] A. Bekasiewicz and S. Koziel, "Miniaturised dual-band branch-line coupler," *Electron. Lett.*, vol. 51, no. 10, pp. 769–771, May 2015.

[24] I. A. Mocanu, "Novel directive coupler with dual band behavior for GSM applications," in *Proc. Int. Symp. Signals, Circuits Syst. (ISSCS)*, Lasi, Romania, Jul. 2015, pp. 1–4.

[25] W. Feng, M. Xun, Y. Zhao, and W. Che, "Dual-band branch line coupler with high isolation isolation using loaded coupled lines," in *Proc. Int. Appl. Comput. Electromagn. Soc. Symp. (ACES)*, Beijing, China, Jul. 2018, pp. 1–2.

[26] B. A. Twumasi and J.-L. Li, "A compact, wideband branch-line balun with small magnitude and phase imbalances," *Electromagnetics*, vol. 39, no. 1, pp. 30–40, Jan. 2019.
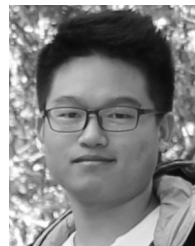
BAIDENGER AGYEKUM TWUMASI received the H.N.D. degree in electrical/electronic engineering from Ho Polytechnic, in 2004, and the M.Sc. degree in telecommunication management from the HAN University of Applied Sciences, The Netherlands, in 2011. He is currently pursuing the Ph.D. degree with the School of Physics, University of Electronic Science and Technology of China, majoring in electronic science and technology. He is also a Lecturer of electrical/electronic engineering at Ho Technical University, Ghana. His research interests include MIMO antenna designs, planar electronic circuits for telecommunication applications, study of electromagnetic time reversal (EMTR) and its applications, wireless power transfer and its related circuits, microwave and millimeter-wave electronic circuits, and systems design, as well as telecommunications management.

LEI XIA received the B.S., M.Sc., and Ph.D. degrees in electronic engineering from the University of Electronic Science and Technology of China (UESTC), Chengdu, China, in 1998, 2004, and 2007, respectively. Since January 2008, he has been with the School of Electronic Science and Engineering, UESTC, where he is currently an Associate Professor. His research interests are microwave and millimeter-wave MCM, LTCC process, and circuits and systems.

JIA-LIN LI received the M.Sc. degree from the University of Electronic Science and Technology of China (UESTC), Chengdu, China, in 2004, and the Ph.D. degree from the City University of Hong Kong, Hong Kong, in 2009, both in electronic engineering. Since September 2009, he has been with the School of Physics, UESTC, where he is currently a Professor. His research interests include microwave/millimeter-wave antenna and arrays, circuits and systems, and interactions between microwave and complex medium.

PENG LIU received the B.S. degree in electronic engineering from the University of Electronic Science and Technology of China (UESTC), Chengdu, China, in 2014, where he is currently pursuing the M.Sc. degree. His research interests include the solid-state-based microwave power combining techniques, and microwave planar passive circuits and components.

SHAN-SHAN GAO received the M.Sc. and Ph.D. degrees from the University of Electronic Science and Technology of China (UESTC), Chengdu, China, in 2008 and 2012, both in electronic engineering. Since July 2013, she has been with the School of Electronic and Information Engineering, Chengdu University, Chengdu, where she is currently an Associate Professor. Her research interests include design and realization of microwave passive devices and circuits and microwave/holographic antennas and arrays.

• • •